# DYNAMIC MODELLING AND IDENTIFICATION OF A COMPACTOR

**É. Guillo, M. Gautier**

*Institut de Recherche en Cybernétique de Nantes, UMR CNRS 6597*
*B.P. 92101, Nantes Cedex 3, France*
*E-mail: Eric.Guillo@ircyn.ec-nantes.fr*

Abstract: This paper deals with the design and identification of the dynamic model of a compactor, an articulated frame steering mobile engine for use in road construction. A classical approach based on an Ordinary Least Squares identification method is used. A survey of these techniques is given and applied to estimate dynamic parameters of the compactor, and especially the contribution of the contact strengths between rolls and soil.

Keywords: Dynamic modelling, identification, Multisensory data fusion, mobile robots.

## 1. INTRODUCTION

The compactor (see Fig. 1) is one of the most important equipment in the set of mobile engines which take part in the area of road construction. A typical use of compactor is in embankment, base and carriageway compaction. It can be seen that the vehicle must follow an efficient trajectory defined in position, velocity and acceleration according to engine degrees of freedom to guarantee the homogeneity and the expected density of considered compacted material. Those features should be improved taking into account a dynamic model compared with a simple path tracking using kinematic model.

There exists many kind of steering systems for earth-moving equipment. According to Dudzinski [2], systematic classification, the compactor (Fig. 1) has an articulated frame steering. Even if such structures are used for a long time (1913), their modelling will be essentially restricted to kinematic one which is based on velocity constraints as pure rolling and non slipping conditions [7].

As the rear and front axles of the compactor are constituted of rigid rolls, the conditions of contact are not similar to a classical wheel interaction with soil. Consequently, a dynamic model that explicitly takes into account bonding strengths is sum up in this paper (See [3] for details). An estimation of the parameters of this model based on an Ordinary Least Squares identification method [6] is given.

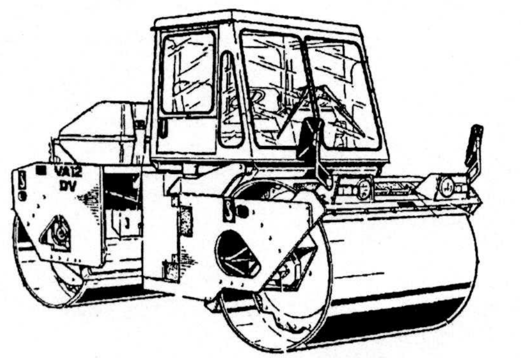


Figure 1. A typical compactor: Albaret VA12 DV.

## 2. DESCRIPTION OF THE COMPACTOR

According to classical robot manipulator description [1], the compactor is considered as a mechanical

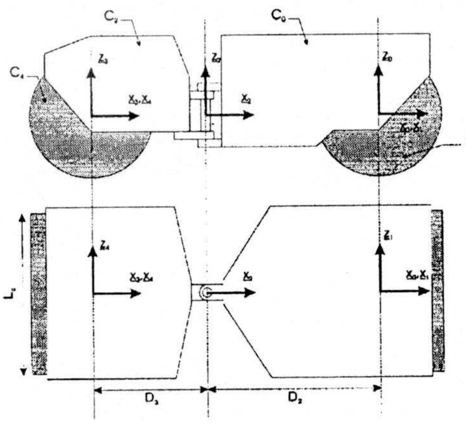

Figure 2. Tree structure of the compactor.

system $\Sigma$ composed of a tree structure of $N$ rigid bodies $C_i$ where $C_0$ is the base body, so that:

$$\Sigma = \bigcup_{i=0}^{N} C_i \qquad N = 4 \tag{1}$$

with the following body definitions (see Fig. 2):

- $C_0$, $C_2$: the front and rear chassis,

- $C_1$, $C_4$: the front and rear rolls,
- $C_3$: a virtual body (used to define a second frame $R_3$ attached to $C_2$).

The system $\Sigma$ is provided with a frame $R_i$ respectively attached to each of the ($N$+1) bodies $C_i$. Let $R_i$ be defined as:

$$R_i = (O_i, \underline{x}_i, \underline{y}_i, \underline{z}_i) \tag{2}$$

### 2.1 Compactor position

**Hypothesis 1.** The compactor moves on the plane $\Pi$ which is perpendicular to the gravity.

Let $R_g$ be a Galilean reference frame attached to the plane $\Pi$ so that:

$$R_g = (O_g, \underline{x}_g, \underline{y}_g, \underline{z}_g) \tag{3}$$

The robot posture can be described by the position and the orientation of the body $C_0$ with respect to the base frame $R_g$. It is given by the following three variables:

- $x_0, y_0$: the coordinates of the reference point $O_0$ in the frame $R_g$,
- $\theta_0$: the orientation of the frame $R_0$ with respect to the frame $R_g$.

### 2.2 Parametrization of the compactor structure

Classical tree structure description using the modified Denavit-Hartenberg notations [5] applied to the system $\Sigma$ defines the geometric parameters of the compactor (see Table 1) with respect to the position and orientation of the body $C_0$.

| $i$ | s | m | $a$ | a | $d$ |
|---|---|---|---|---|---|
| 1 | 0 | 1 | 0 | $-\pi/2$ | 0 |
| 2 | 0 | 1 | 0 | 0 | $-D_2$ |
| 3 | 2 | 0 | 2 | 0 | $-D_3$ |
| 4 | 0 | 1 | 3 | $-\pi/2$ | 0 |

Table 1. Geometric parameters of the compactor

In that case the homogeneous transform (4) of the frame $R_i$ relative to $R_{ai}$ (where $a_i$ is the antecedent of $i$) is expressed as a function of the 4 following parameters:

- $\alpha_i$: angle between $\underline{z}_{a_i}$ and $\underline{z}_i$, corresponding to a rotation about $\underline{x}_{a_i}$,
- $d_i$: distance from $\underline{z}_{a_i}$ to $\underline{z}_i$ along $\underline{x}_{a_i}$,
- $\theta_i$: angle between $\underline{x}_{a_i}$ and $\underline{x}_i$, corresponding to a rotation about $\underline{z}_i$,
- $r_i$: distance from $\underline{x}_{a_i}$ to $\underline{x}_i$ along $\underline{z}_i$.

$$^{a_i}\underline{\underline{Z}}_i = \begin{bmatrix} ^{a_i}\underline{\underline{A}}_i & ^{a_i}\underline{P}_i \\ 0_{1\times 3} & 1 \end{bmatrix} \quad \text{with } ^{a_i}\underline{\underline{A}}_i = \begin{bmatrix} ^{a_i}\underline{s}_i & ^{a_i}\underline{n}_i & ^{a_i}\underline{k}_i \end{bmatrix} \tag{4}$$

where $^{a_i}\underline{\underline{A}}_i$ is the $(3\times 3)$ rotation matrix which defines the orientation of the frame $R_i$ with respect to the frame $R_{ai}$ and $^{a_i}\underline{P}_i$ is the origin of the frame $R_i$ expressed in the frame $R_{ai}$.

**Remark 1.** $\mu_i = 1$ means that the $i$-joint is actuated and $\mu_i = 0$ that it is not. $\sigma_i$ specifies the type of the joint ($\sigma_i = 0$ if rotational, $\sigma_i = 1$ if translational, $\sigma_i = 2$ if fixed).

### 2.3 Generalized coordinates

According to the previous description of the compactor, the vehicle motion is completely described by the following vector of $(n = 6)$ generalized coordinates:

$$q(t) = \begin{bmatrix} x_0 \; y_0 \; \theta_0 \; \theta_1 \; \theta_2 \; \theta_4 \end{bmatrix}^T \tag{5}$$

This description can be easily applied to other articulated frame steering engine like: double-jointed loader, loader with articulated pendulum joint and so on. On the other hand expressions of kinetic and potential energies using this description are well known for a while now.

## 3. DYNAMIC MODELLING

Let $\Sigma$ be the mechanical system where position is given by the vector of parameters $q$ and $L_\Sigma$ its Lagrangian. Let $\underline{\tau}$ (of same dimension as $q$) be the vector of the generalized forces applied to the system $\Sigma$. Then the vector $q$ satisfies the following system of Lagrange equations:

$$\frac{d}{dt}\left(\frac{\partial}{\partial \dot{q}}(L_\Sigma)\right) - \frac{\partial}{\partial q}(L_\Sigma) = \underline{\tau} \tag{6}$$

When the Lagrange equations are calculated for the system $\Sigma$, they yield a dynamic equation which can be written in the form:

$$\underline{\underline{M}}(q)\cdot\ddot{q} + \underline{H}(q, \dot{q}) = \underline{\tau} \tag{7}$$

where

- $\underline{\underline{M}}(q)$ is the $(n\times n)$ mass matrix of the system $\Sigma$
- $\underline{H}(q, \dot{q})$ is a $(n\times 1)$ vector of centrifugal and Coriolis terms.

The statement of forces acting on the system $\Sigma$ is divided in two parts:

$$\underline{\tau} = \underline{U} + \underline{Q} \tag{8}$$

where $\underline{U}$ depends on the motor torques on joints 1, 2 and 4 as shown in table 1 and $\underline{Q}$ on the bonding strengths between the plan $\Pi$ and the rolls $C_1$ and $C_4$. The development of the vector $\underline{\tau}$ gives

$$\underline{U} = \begin{bmatrix} 0 & 0 & 0 & u_1 & u_2 & u_4 \end{bmatrix}^T \quad (9)$$

where $u_i$ is the motor torque on $i$-joint and

$$\underline{Q} = \sum_i \underline{\underline{K}}_i \cdot {}^{a_i}\underline{\mathfrak{I}}^{O_i}_{\Pi \to C_i} \qquad i = 1, 4 \quad (10)$$

where $\underline{\mathfrak{I}}^{O_i}_{\Pi \to C_i}$ points out the wrench of the resultant bonding strengths at point $O_i$. Its expression projected in frame $R_{ai}$ gives:

$$ {}^{a_i}\underline{\mathfrak{I}}^{O_i}_{\Pi \to C_i} = \begin{bmatrix} S^i_x \\ S^i_y \\ S^i_z \\ 0 \\ -R_c \cdot S^i_x \\ -T^i_z \end{bmatrix} \text{ with } \begin{cases} S^i_x = \int_{\Delta_i} F^{D_i}_x(l) dl \\ S^i_y = \int_{\Delta_i} F^{D_i}_y(l) dl \\ S^i_z = \int_{\Delta_i} F^{D_i}_z(l) dl \\ T^i_z = \int_{\Delta_i} (l \cdot F^{D_i}_x(l)) dl \end{cases} \quad (11)$$

where

$$\begin{cases} F^{D_i}_x(l) = \underline{F}^{D_i}_{\Pi \to C_i}(l) \cdot \underline{x}_{a_i} \\ F^{D_i}_y(l) = \underline{F}^{D_i}_{\Pi \to C_i}(l) \cdot \underline{y}_{a_i} \\ F^{D_i}_z(l) = \underline{F}^{D_i}_{\Pi \to C_i}(l) \cdot \underline{z}_{a_i} \end{cases} \quad (12)$$

On the other hand the $(n \times 6)$ matrix $\underline{\underline{K}}_i$ has the following definition

$$\underline{\underline{K}}^T_i = \begin{bmatrix} \frac{\partial}{\partial \dot{q}}\left({}^{a_i}\underline{V}^{O_i}_{C_i, \Pi}\right) \\ \frac{\partial}{\partial \dot{q}}\left({}^{a_i}\underline{\omega}_{C_i, \Pi}\right) \end{bmatrix} \qquad i = 1, 4 \quad (13)$$

where ${}^{a_i}\underline{V}^{O_i}_{C_i, \Pi}$ is the velocity of the point $O_i$ of the body $C_i$ relative to the plane $\Pi$ expressed in the frame $R_{ai}$ and where $\underline{\omega}_{C_i, \Pi}$ is the rotation velocity of the body $C_i$ relative to the plane $\Pi$.

As a result, the new expression of the dynamic model of the compactor is given by:

$$\underline{\underline{M}}(q)\ddot{q} + \underline{H}(q, \dot{q}) = \underline{U} + \underline{\underline{K}}_1 \cdot {}^{0}\underline{\mathfrak{I}}^{O_1}_{\Pi \to C_1} + \underline{\underline{K}}_4 \cdot {}^{3}\underline{\mathfrak{I}}^{O_4}_{\Pi \to C_4} \quad (14)$$

where $\underline{\underline{M}}(q)$, $\underline{H}(q, \dot{q})$, $\underline{U}$ and $\underline{\underline{K}}_i$ are known matrices. On the other hand, the wrench of the resultant strengths ${}^{a_i}\underline{\mathfrak{I}}^{O_i}_{\Pi \to C_i}$ has to be determined.

### *3.1 The roll-soil interaction model*

The simplified roll-soil interaction model on the figure (3) is used to determine the expression of $\underline{\mathfrak{I}}^{O_i}_{\Pi \to C_i}$ that points out the wrench of the resultant bonding strengths at point $O_i$.

In these conditions the roll $C_i$ is in permanent contact with the soil along a surface $S_i$ which represents an angular part $\varphi_0$ of its circumference.

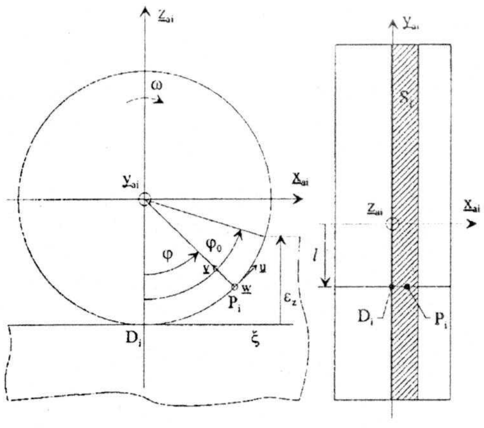


Figure 3: Simplified roll-soil interaction model.

Let $P_i$ be a point of the surface $S_i$.

**Remark 2.** $(\xi, \eta)$ are used to specify the relative co-ordinates of a point of the contact surface $S_i$ (see Fig. 3):

$$\begin{aligned} \xi &= R_c(\varphi_0 - \varphi) \qquad \xi \in [0, \xi_s = R_c\varphi_0] \\ \eta &= l \qquad \eta \in [-L_c/2, L_c/2] \end{aligned} \quad (15)$$

**Hypothesis 2.** The depression $\varepsilon_z$ in the ground is small compared to the radius $R_c$ of the rolls: $\varepsilon_z \ll R_c$.

According to the hypothesis (2), it is possible to simplify the expression of the longitudinal shear displacement $\Delta\xi$ and $\Delta\eta$ the transversal shear displacement to obtain (see Rem. 2):

$$\begin{aligned} \Delta\xi &= g_x \xi \\ \Delta\eta &= g_y \xi \end{aligned} \quad (16)$$

where the longitudinal slip $g_x$ and the transversal slip $g_y$ are defined as following:

$$\begin{aligned} g_x &= \frac{V_x - l\dot{\theta} - R_c\omega}{R_c\omega} \\ g_y &= \frac{V_y}{R_c\omega} \end{aligned} \quad (17)$$

$$\text{with } {}^{a_i}\underline{V}^{O_i}_{C_i, \Pi} = \begin{bmatrix} V_x \\ V_y \\ 0 \end{bmatrix} \quad {}^{a_i}\underline{\omega}_{C_i, \Pi} = \begin{bmatrix} 0 \\ \omega \\ \dot{\theta} \end{bmatrix} \quad {}^{a_i}\underline{O_i P_i} = \begin{bmatrix} R_c \sin\varphi \\ l \\ -R_c \cos\varphi \end{bmatrix}$$

When a torque is applied to a roll, shearing action is initiated on the vehicle running gear-terrain interface. To predict vehicle thrust and associated slip, the shear stress-shear displacement relationship of the terrain is required.

Based on a considerable amount of field data, it is found that there are three types of shear stress-shear displacement relationship commonly observed [8]. In the case of the compactor this relationship exhibits

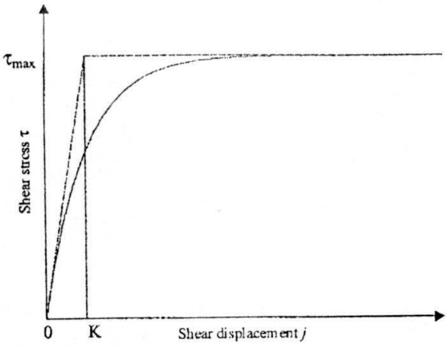


Figure 4: The shear stress-shear displacement relationship

characteristics shown in (Fig. 4). It may be described by an exponential function of the following form:

$$\begin{aligned}\tau &= \tau_{max}(1 - e^{-j/K}) \\ &= (c + \sigma \tan\phi)(1 - e^{-j/K})\end{aligned} \tag{18}$$

where

- $\tau$ is the shear stress,
- $j$ is the shear displacement,
- $c$ and $\phi$ are the cohesion and the angle of internal shearing resistance of the terrain,
- $K$ is the shear deformation modulus,
- $\sigma$ is the normal pressure.

### 3.2 Characterization of the shear stress-slip relationship

**Hypothesis 3.** The pressure distribution $F_z$ along the contact patch $S$ is uniform and equal to

$$F_z = W/(L_c\xi_s) \tag{19}$$

**Hypothesis 4.** The shear stress-shear displacement relationship (18) used for small shear displacement can be simplified as following

$$\tau = \tau_{max} \cdot j/K \qquad j \le K \tag{20}$$

According to the expression of the longitudinal and transversal shear displacements (16), the shear stress at point $D_i$ is written

$$\tau = \tau_{max} \cdot \sqrt{\Delta\xi^2 + \Delta\eta^2}/K \qquad \sqrt{\Delta\xi^2 + \Delta\eta^2} \le K \tag{21}$$

Let $\beta$ be the slip angle at point $D_i$. Then the longitudinal and transversal components of the shear stress are

$$\begin{aligned}\tau_\xi &= \tau\cos\beta = \tau g_x(g_x^2 + g_y^2)^{-1/2} \\ \tau_\eta &= \tau\sin\beta = \tau g_y(g_x^2 + g_y^2)^{-1/2}\end{aligned} \tag{22}$$

### 3.3 Longitudinal and transversal efforts

The longitudinal and transversal efforts are determined using the spatial integration of the shear stress along the contact patch between the roll and the terrain. In these conditions the longitudinal effort $F_x$ at point $D_i$ is written as

$$\begin{aligned}F_x^{D_i}(l) &= \int_0^{\xi_s} \tau_\xi d\xi \\ &= \int_0^{\xi_s} \tau_{max} g_x \frac{\xi}{K} d\xi\end{aligned} \tag{23}$$

Assuming that the hypothesis (3) is verified it gives

$$F_x^{D_i}(l) = \tau_{max} g_x \frac{\xi_s^2}{2K} \tag{24}$$

In the same way, the transversal effort $F_y$ is calculated

$$F_y^{D_i}(l) = \tau_{max} g_y \frac{\xi_s^2}{2K} \tag{25}$$

### 3.4 The case of the straight line

Relations (14, 11, 13, 24, 25) gives the general expression of the dynamic model according to the selected roll-soil interaction model. To verify the hypotheses given below, the identification process had been performed along the most simple trajectory: a straight line.

In these conditions, the dynamic model has the following simplified expression:

$$\begin{cases} M\ddot{x}_0 = K_{x1}g_{x1} + K_{x4}g_{x4} \\ ZZ_1\ddot{\theta}_1 + F_{v1}\dot{\theta}_1 + F_{s1}\operatorname{sgn}\dot{\theta}_1 = u_1 - R_cK_{x1}g_{x1} \\ ZZ_4\ddot{\theta}_4 + F_{v4}\dot{\theta}_4 + F_{s4}\operatorname{sgn}\dot{\theta}_4 = u_4 - R_cK_{x4}g_{x4} \end{cases} \tag{26}$$

where

- $M$ is the total mass of the compactor,
- $ZZ_i(i = 1, 4)$ is the inertia of the roll $C_i$,
- $K_{xi}(i = 1, 4)$ is the coefficient of bonding strengths for the $i$-joint,
- $F_{vi}(i = 1, 4)$ is the viscous friction parameter for the $i$-joint,
- $F_{si}(i = 1, 4)$ is the striction friction parameter for the $i$-joint.

## 4. IDENTIFICATION MODEL

### 4.1 Standard dynamic parameters

The relation (26) is linear in relation to a set of $(n_p = 9)$ parameters, $X_s$.

$$Y_s = D_s(\dot{q}, \ddot{q}, g_{x1}, g_{x4}) \cdot X_s \qquad (27)$$

with

$$Y_s = \begin{bmatrix} 0 \\ u_1 \\ u_4 \end{bmatrix}$$

$$D_s = \begin{bmatrix} \ddot{x}_0 & 0 & 0 & 0 & -g_{x1} & 0 & 0 & 0 & -g_{x4} \\ 0 & \ddot{\theta}_1 & \dot{\theta}_1 & \operatorname{sgn}\dot{\theta}_1 & R_c g_{x1} & 0 & 0 & 0 & 0 \\ 0 & 0 & 0 & 0 & 0 & \ddot{\theta}_4 & \dot{\theta}_4 & \operatorname{sgn}\dot{\theta}_4 & R_c g_{x4} \end{bmatrix}$$

$$X_s = \begin{bmatrix} M & ZZ_1 & F_{v1} & F_{s1} & K_{x1} & ZZ_4 & F_{v4} & F_{s4} & K_{x4} \end{bmatrix}^T$$

$D_s$ is the $(n_e \times n_p)$ regressor of the linear dynamic identification model, which can be used to identify the standard dynamic parameters, $X_s$ ($n_e = 2$, the number of equations in $D_s$).

### 4.2 Sensors influence on modelling

Each roll of the compactor is equipped with an hydraulic actuator. Two sensors are used to measure the pressure in each chamber of the actuator to determine the motor torque. They introduce systematic error on load pressure due to the presence of offset on each measurement. Consequently, the dynamic model (27) is modified to take into account these observations as follows:

$$u_{1m} = u_1 + u_{10} \qquad (28)$$

where:

$u_{im}$, $u_i$, $u_{i0}$ respectively are measured, literal and offset values of motor torque on the $i$-joint.

So the new dynamic model deduced from (27) and (28) gives:

$$Y_s = D_s(\dot{q}, \ddot{q}, g_{x1}, g_{x4}) \cdot X_s \qquad (29)$$

with

$$Y_s = \begin{bmatrix} 0 \\ u_1 \\ u_4 \end{bmatrix}$$

$$D_s = \begin{bmatrix} \ddot{x}_0 & 0 & 0 & 0 & -g_{x1} & 0 & 0 & 0 & 0 & -g_{x4} & 0 \\ 0 & \ddot{\theta}_1 & \dot{\theta}_1 & \operatorname{sgn}\dot{\theta}_1 & R_c g_{x1} & 1 & 0 & 0 & 0 & 0 & 0 \\ 0 & 0 & 0 & 0 & 0 & 0 & \ddot{\theta}_4 & \dot{\theta}_4 & \operatorname{sgn}\dot{\theta}_4 & R_c g_{x4} & 1 \end{bmatrix}$$

$$X_s = \begin{bmatrix} M & ZZ_1 & F_{v1} & F_{s1} & K_{x1} & u_{10} & ZZ_4 & F_{v4} & F_{s4} & K_{x4} & u_{40} \end{bmatrix}^T$$

### 4.3 Identification method

Parameters are estimated as the Ordinary Least Squares (OLS) solution of an overdetermined linear system of $r$ equations in $n_p$ unknowns, obtained from the sampling of the dynamic model along a known trajectory $(\dot{q}, \ddot{q}, g_{x1}, g_{x4})$:

$$Y = W_s \cdot X_s + \rho \qquad (30)$$

with:

$$Y = \begin{bmatrix} Y^{(1)} \\ \vdots \\ Y^{(n_e)} \end{bmatrix} \qquad Y^{(j)} = \begin{bmatrix} Y^{(j)}(1) \\ \vdots \\ Y^{(j)}(n_s) \end{bmatrix}$$

$$W_s = \begin{bmatrix} D_s^{(1)} \\ \vdots \\ D_s^{(n_e)} \end{bmatrix} \qquad Y^{(j)} = \begin{bmatrix} D_s^{(j)}(1) \\ \vdots \\ D_s^{(j)}(n_s) \end{bmatrix}$$

where:

- $W_s$ is the $(r \times n_p)$ observation matrix,
- $n_s$ is the number of samples,
- $r$ is the number of equations $(r = n_e \cdot n_s > n_p)$.

The Least Squares (LS) solution $X_s$ minimizes the 2-norm of the error vector $\rho$ in (30):

$$\hat{X_s} = min_{X_s} \|W_s \cdot X_s - Y\|_2 \qquad (31)$$

## 5. PRACTICAL IMPLEMENTATION

### 5.1 Dynamic identification

Measurements of six signals are used to carry out the identification of the dynamic parameters of the compactor:

- $\theta_1$, a precision encoder $(4 \times 2048(pt/rev))$ on $C_1$
- $\theta_4$, a precision encoder $(4 \times 2048(pt/rev))$ on $C_4$
- $u_1, u_4$, two pressure sensors $(0, 10V)(0, 400bars)$

On the other hand, a free bicycle wheel equipped with a precision encoder $(4 \times 4096(pt/rev))$ is fixed on each side of the front roll. The resultant data are two rotation angles $\theta_l$ and $\theta_r$. Knowing the wheel radii $R_l$ and $R_r$ and the distances from the wheels to the roll centre $D_l$ and $D_r$, the translation and rotation speed of the front roll are given by the equations of the unicycle:

$$\begin{bmatrix} \underline{V}_{O_1}^{C_1, \Pi} \cdot x_0 \\ \underline{\omega}_{C_1, \Pi} \cdot z_0 \end{bmatrix} = \frac{1}{D_l + D_r} \cdot \begin{bmatrix} D_r \cdot R_l & D_l \cdot R_r \\ -R_l & R_r \end{bmatrix} \cdot \begin{bmatrix} \dot{\theta}_l \\ \dot{\theta}_r \end{bmatrix} \qquad (32)$$

The relation (32) supposes that each of the two bicycle wheels satisfies the non slipping condition.

Low-pass filtering associated with a central differentiation algorithm provides a digital pass-band filter to estimate derivatives at low frequencies and to decrease high frequency noise which comes from numerical differentiation.

After calculating $Y$ and $W_s$ to get (30), $Y$ and all column of $W_s$ are low-filtered in a process called parallel filtering to eliminate high-frequency noise. Estimated value of dynamic parameters $X_s$ are given in table 2 with their relative standard deviations:

$$\hat{\sigma}_r = \frac{\hat{\sigma}_{\hat{X}_s}}{\hat{X}_s} \qquad i = 1, \ldots, n_p \qquad (33)$$

| Parameters | Units | $\hat{X}_s$ | $\hat{\sigma}_r$ (%) |
|---|---|---|---|
| $M$ | kg | - | - |
| $ZZ_1$ | kg.m² | 556.32 | 0.29 |
| $F_{v1}$ | Nm.s$^{-1}$ | 64.75 | 3.89 |
| $F_{s1}$ | Nm | 174.74 | 2.65 |
| $K_{x1}$ | N | -259.82 | 26.64 |
| $u_{10}$ | Nm | -183.14 | 0.95 |
| $ZZ_4$ | kg.m² | 671.33 | 0.3 |
| $F_{v4}$ | Nm.s$^{-1}$ | 82.84 | 3.1 |
| $F_{s4}$ | Nm | 142.73 | 3.33 |
| $K_{x4}$ | N | -309.59 | 17.24 |
| $u_{40}$ | Nm | -181.94 | 0.95 |

Table 2. Identified dynamic parameters

with:

$$cond(W_s) = 81,58$$
$$cond(\Phi) = 94,52 \qquad \Phi = W_s \cdot diag(\hat{X}_s) \qquad (34)$$

The trajectories used to identify dynamic parameters of the compactor are not enough exciting. That is why all the parameters are not well estimated (especially the total mass $M$ of the compactor). On the other hand, according to data from Albaret, the estimated value of roll inertia are satisfying.
More exciting trajectories are now used to perform a better identification. Results are expected soon.

# 6. CONCLUSION

In this paper, the dynamic model of a compactor which explicitly includes bonding strengths with soil was presented. In order to describe the configuration of an articulated frame steering mobile engine, a parametrization using classical robot description was proposed. The results clearly show that the slip is essential and must be taken into account particularly during cornering.

## Acknowledgements

This paper presents research results managed in collaboration with the LCPC (Laboratoire Central des Ponts et Chaussées, France). The authors would like to thank François Peyret for fruitful discussions concerning the area of road construction and Michel Froumentin for his inestimable help during trials.

# REFERENCES

[1] Canudas de Wit C., B. Siciliano and G. Bastin (1997). In: *Theory of Robot Control*, 2nd printing, Chap. 1, pp. 4-29, Springer-Verlag, London.
[2] Dudzinski P.A. (1989). Design characteristics of steering systems for mobile wheeled earth-moving equipment. *Journal of Terramechanics*, **vol. 26, no. 1**, pp. 25-82.
[3] Guillo E., M. Gautier and F. Boyer (1999). Dynamic modelling and simulation of a compactor. In: *Proceedings of 14th IFAC World Congress*, Beijing, China.
[4] Khalil W. and D. Creusot (1997). SYMORO+: A system for the symbolic modelling of robots. *Robotica*, **vol. 15**, pp. 153-161.
[5] Khalil W. and J.-F. Kleinfinger (1986). A New Geometric Notation for Open and Closed-loop Robots. In: *Proceedings of IEEE International Conference on Robotics and Automation*, San Francisco, California, pp. 1174-1180.
[6] Lawson C.L. and R.J. Hanson (1974). *Solving Least Squares Problems*. Englewood Cliffs, Prentice Hall edition.
[7] Tilbury D., O. Sordalen, L. Bushnell and S. Sastry (1994). A multi-steering trailer system: conversion into chained form using dynamic feedback. In: *Preprints of the 4th IFAC Symposium on Robot Control*, Capri, Italy, pp. 159-164.
[8] Wong J.Y. (1993). *Theory of ground vehicles*. 2nd edition, John Wiley & Sons Inc., pp. 77-167.